Mass Spectrometry

DOI: 10.1002/anie.200604468

The Chemical Composition of Animal Cells and Their Intracellular Compartments Reconstructed from 3D Mass Spectrometry**

Daniel Breitenstein, Christina E. Rommel, Rudolf Möllers, Joachim Wegener, and Birgit Hagenhoff*

Experimental approaches for analyzing the chemical composition of animal cells with spatial resolution are important for many fields of biomedical research. The analysis of three-dimensional microstructures by time-of-flight secondary-ion mass spectrometry (TOF-SIMS) is an emerging technique to make the molecular architecture of biological samples accessible. In SIMS the sample surface is bombarded by primary ions. A fraction of the energy transported in the so-called collision cascade is directed back to the sample surface and causes the desorption of neutral and charged chemical species (secondary ions) from the uppermost molecular layer. These are subsequently collected and analyzed with respect to their mass/charge ratio.[1] Today, most state-of-the-art instruments for organic applications use TOF analyzers for mass determination of the desorbed secondary ions.[2] TOF-SIMS allows the detection of all elements as well as small organic molecules in parallel and has a sensitivity down to the ppm/femtomole range.[3] Scanning the sample surface with the primary-ion beam provides a 2D image of the chemical surface composition. Moreover, prolonged ion bombardment of the sample at a constant position leads to sputter erosion. Mass analysis of the sputtered material then reveals the vertical composition of the sample.[1] The lateral distribution of organic material can be imaged with a resolution of about 150–400 nm,[4–6] whereas the vertical resolution in organic polymer films was shown to be better than 30 nm.[7]

Application to biological samples like cells and tissues, however, has so far been hindered by the limited signal intensities obtained from organic materials and the fact that the collision cascade destroys organic molecules and, thus, molecular information. The low signal intensities in surface analysis and the loss of molecular information in sputter depth profiling have been improved by the use of polyatomic primary ions like Au_3^+ and Bi_3^+.[3,8] Moreover, buckminsterfullerenes have become available as a new ion source for sputter erosion.[9] The impact of C_{60}^+ ions was found to be less destructive to organic samples than the common sputter ions O_2^+ and Cs^+.[10] Even intact organic molecules survive the sputter process.[11] Thus, it was the objective of this study to reconstruct the molecular composition of animal cells in three dimensions by applying repeated cycles of SIMS analysis of the sample surface followed by sputter erosion that exposes a deeper layer of the sample to the next round of SIMS analysis (TOF-SIMS 3D microarea analysis). In a dual-beam setup Bi_3^+ primary ions were used to determine the chemical composition of the surface, and C_{60}^+ ions were used for intermittent sputter erosion.[12]

Six confluent layers of normal rat kidney (NRK) cells, grown on cover slips under ordinary cell-culture conditions, were analyzed by TOF-SIMS 3D microarea analysis after the cells had been stabilized by chemical fixation. Chemical fixation is a routine procedure to preserve the structure of biological samples in high vacuum.[13] TOF-SIMS results were very reproducible and similar for all samples so that data presentation here is confined to one typical experiment.

Figure 1 illustrates a unique aspect of TOF-SIMS microarea analysis that is very different from optical-image acquisition. At the beginning of the experiment a confluent cell layer is present on the culture substrate. The uppermost molecular layer (thick line in Figure 1a) accessible for SIMS will consist of chemical species originating from the cell surfaces. During intermittent sputter cycles the sample sur-

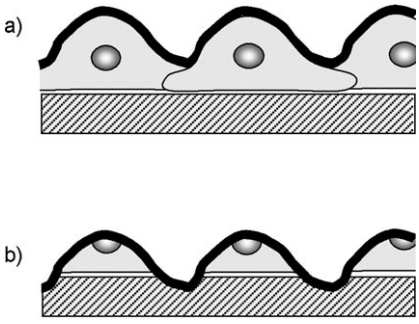

Figure 1. Confluent cells on a growth substrate at the beginning (a) and in the middle (b) of a TOF-SIMS sputter erosion experiment assuming constant sputter rates for all materials. The thick line represents the uppermost molecular layer imaged in SIMS.

[*] Dr. C. E. Rommel, PD Dr. J. Wegener
Institut für Biochemie
Westfälische Wilhelms-Universität Münster
Wilhelm-Klemm Strasse 2, 48149 Münster (Germany)
Fax: (+49) 251-833-3206
E-mail: wegenej@uni-muenster.de
Dr. D. Breitenstein, Dr. B. Hagenhoff
Tascon GmbH
Heisenbergstrasse 15, 48149 Münster (Germany)
Dr. R. Möllers
IonTof GmbH
Heisenbergstrasse 15, 48149 Münster (Germany)

[**] This study was financially supported by the German Ministry for Education and Research (BMBF) under grant number 0312002A (Nanobiotechnology) and the European Union under grant numbers FP6-513698 (Toxdrop) and FP6-005045 (Nanobiomaps). The authors acknowledge the help of M. Fartmann for careful revision of the manuscript, S. Grunewald for her expert help with the cell cultures, and both R. Kersting and E. Tallarek for technical advice. We also thank E. Niehuis for helpful discussions and J. Zehnpfenning for providing software support.

face will be gradually eroded. As the cell bodies are not evenly thick, SIMS analysis will reach the growth surface in the cell periphery after fewer sputter cycles than in the cell centers (Figure 1b). The resulting distortion along the z axis can be corrected by mathematical deconvolution.

Figure 2a–c compares secondary-ion images originating from the surface of a confluent monolayer of NRK cells before any sputter cycle had been applied (compare Figure 1a). Figure 2a shows the lateral distribution of the sodium signal representing the glass substrate; the silicon signal is not unique at nominal mass resolution but overlaps with organic fragments. Figure 2b provides the lateral intensity distribution of a signal pooled from a set of peaks that were assigned to amino acid fragments. Similarly Figure 2c shows the intensity distribution of a pool of secondary ions assigned to phospholipids. Reference spectra were recorded at high mass resolution from pure amino acids, peptides, proteins, and phospholipids in order to back up peak assignment. Individual mass/charge ratios pooled to either amino acids or phospholipids are specified in the legend of Figure 2.

Before any sputter erosion the uppermost monolayer of the sample does not show any signals of the glass substrate (Figure 2a), indicating that the surface is completely covered by organic material. The lateral distribution of phospholipids is intense but laterally homogeneous without contrast and visible cell margins (Figure 2c). The image reconstructed for amino acids (Figure 2b) is less intense than the one for phospholipids and does not show any structural landmarks anticipated for the surface of the cellular plasma membrane on this scale.

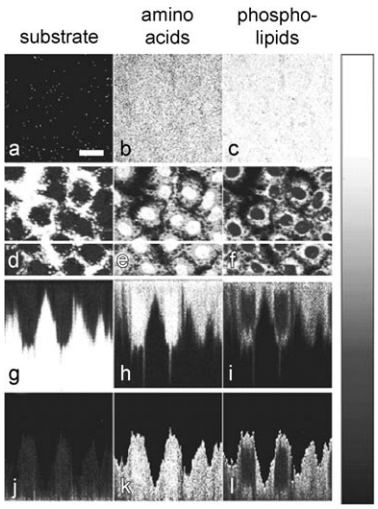

Figure 2. Mass-resolved secondary-ion images of the sample surface before any sputter cycle had been applied (a–c) and within the cell after the 45th sputter cycle (d–f). Image intensities are color coded on a black-and-white scale with white corresponding to high intensities. The color scale is normalized to the intensity in the brightest pixel. The scale bar in (a) corresponds to 20 μm. g)–i) *xz* Sections through the three-dimensional data stack along the white line in (d)–(f). Parts (j)–(l) show the data of parts (g)–(i) after a mathematical correction of the *z* axis. Mass-resolved images are based on the following secondary ions: (a), (d), (g), (j): Na^+; (b), (e), (h), (k): amino acid fragment ions (pooled signal for masses 30 u, 44 u, 70 u, 101 u, 110 u, 136 u); (c), (f), (i), (l): phospholipid fragment ions (pooled signal for masses 58 u, 166 u, 184 u, 760 u).

In secondary-ion images of the cell layer recorded after 45 sputter cycles (Figure 2d–f, situation as in Figure 1b) the signal of the growth substrate shows high intensities in the peripheral, thinner parts of the cells (Figure 2d). The organic material has been completely eroded here. In more central parts of the cell bodies TOF-SIMS data provide label-free molecular information from the inside of the cell. Phospholipid-derived signals (Figure 2f) are detectable with highest intensities in ring-shaped structures around a central compartment mainly devoid of phospolipids but enriched in amino acids (Figure 2e). With respect to intracellular location, chemical composition, and dimensions this central compartment corresponds to the cell nucleus.[14] These intense amino acid signals in the nucleus may be based on the dense packing of histone proteins that spool and compact the DNA. Consistently Arlinghaus et al. found by laser secondary-neutral mass spectrometry applied to animal tissue after cryofixation that a central part of the cells opened by microtome cutting was rich in nitrogen-containing fragments, whereas the outer area of the cell was found to be rich in phospholipid-derived signals.[15] Moreover, in dynamic SIMS imaging the cell nucleus was identified by high-intensity signals of nitrogen-containing hydrocarbons.[16] The lateral distribution of pooled phospholipid signals (Figure 2f) implies that the signal arises from both inner (endo) and outer (exo) membranes of the cell.

TOF-SIMS 3D microarea analysis provides a wealth of data. In the experiments described here the sample was scanned using 256×256 pixels at 97 individual z levels, yielding a total of more than 6 million volume pixels (voxels). The total data set of a single experiment comprises a complete mass spectrum for each of the individual voxels (here at nominal mass resolution only). Based on this pool of data recorded in subsequent imaging/sputter cycles, it is also possible to reconstruct the vertical distribution of a fragment ion (perpendicular to the sample surface). Figure 2g–i compares the vertical distributions (xz sections) of the classes of compounds discussed above within a plane that runs along the white line indicated in Figure 2d–f and perpendicular to the sample surface. Owing to the peculiarities of 3D microarea analysis (see Figure 1) this representation does not provide a true z axis. Instead, the number of applied sputter cycles increases in direction from the upper to the lower border of either image. In order to present the data on a deconvoluted z axis, Figure 2g–i has been transformed to Figure 2j–l. This computational transformation uses the rather sharp edge between high and low intensities of the substrate signal along the x direction in Figure 2g as a baseline ($z = 0$), and the z positions of all other pixels were expressed relative to this baseline. As a result the images in Figure 2j–l provide realistic side views of the sample on a flat surface. Please note that no correction for inhomogeneous sputter yields was applied. The z axis is therefore somewhat distorted due to material-dependent sputter yields.

Signals originating from the growth substrate (Figure 2j) are consistently restricted to the bottom part of the xz section. Phospholipid signals (Figure 2l) are mainly detected in ring-shaped structures that circumscribe the cell bodies as expected for plasma membrane constituents. The intracellular

compartment that is enriched in amino acids (Figure 2k) corresponds to the cell nucleus. The lateral dimensions of cell body and nucleus correspond favorably to the values that we determined from light-microscopy images (diameter of the cell body ≈20 μm; diameter of the nucleus 10–12 μm). It is important to emphasize that in TOF-SIMS 3D microarea analysis the molecular information is provided without the need to label a subset of chemical species like, for instance, in fluorescence microscopy.

Figure 3 provides a correlation analysis of the data presented in Figure 2d–f. The individual spatial distributions of substrate-derived, amino acid derived, and phospholipid-derived secondary ions inside the sample are shown in Figure 3a–c. Figure 3d shows the overlay of all three signal intensities. When members of the two secondary-ion groups co-localize, the pixel is shown in the corresponding mixed color. This type of representation makes it possible to identify co-localizations of different chemical species. This is also possible by fluorescence microscopy, but the present method is not restricted by the availability of fluorophores with suitable absorption and emission properties. Figure 3e,f shows RGB overlays for an *xz* section through the sample in original presentation and after transformation of the *z* axis, respectively, as described above. These multicolor images correctly visualize the well-known molecular composition of animal cells and can now be applied to other molecules of interest that have an unknown distribution inside the cell as long as their secondary ions are detectable by TOF-SIMS.

Figure 4 shows a typical mass spectrum recorded after 45 sputter cycles representing the situation imaged in Figure 2d,e (recorded in high-mass-resolution mode). In the higher mass range the most dominant peaks can be assigned to phospholipids and cholesterol. Both the phospholipid palmitoyloleyl-phosphatidylcholine (POPC) and cholesterol can be detected as intact molecular ions, whereas the amino acids are predominantly identified by their fragment ions. Peak assignments were confirmed by comparison with reference spectra recorded with the pure substance. The mass spectrum verifies that the repeated C_{60}^+ sputter cycles do not destroy all molecular information on the sample surface.

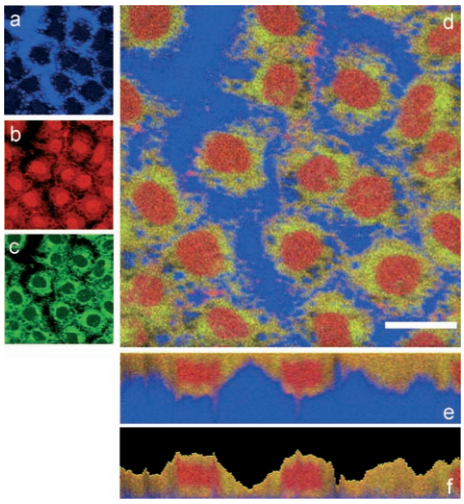

Figure 3. Red–green–blue color overlay for correlation analysis of the data presented in Figure 2d–i. Pooled signals of amino acid fragment ions are represented in red (b), those of phospholipids in green (c), and substrate-derived secondary ions are depicted in blue (a). The scale bar in (d) corresponds to 20 μm. a)–d) Horizontal *xy* sections and e), f) vertical *xz* sections through the sample. For details see text.

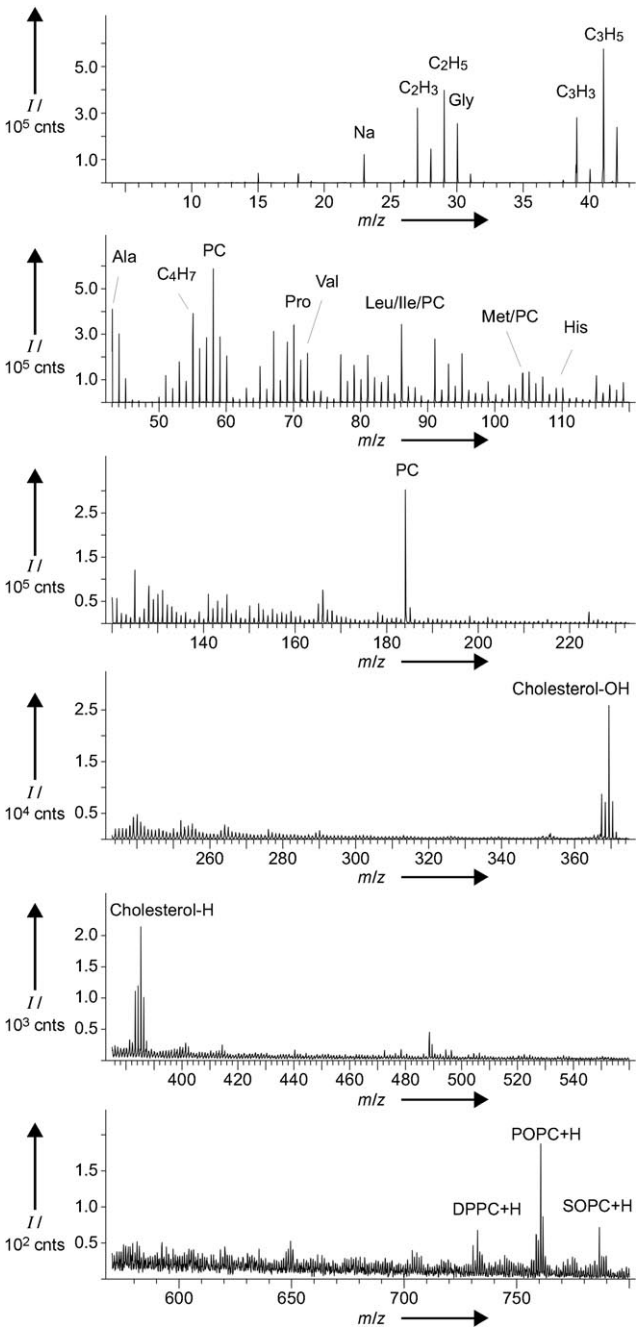

Figure 4. Secondary-ion spectrum (positive polarity) recorded in high-mass-resolution mode in a sputter crater after the 45th sputter cycle. Gly: glycine, Ala: alanine, PC: various phosphatidylcholine fragments, Pro: proline, Val: valine, Leu: leucine, Ile: isoleucine, Met: methionine, His: histidine, DPPC: dipalmitoyl-phosphatidylcholine, POPC: palmitoyl-oleyl-phosphatidylcholine, SOPC: stearyl-oleyl-phosphatidylcholine.

The chemical composition of animal cells can be reconstructed in three dimensions by TOF-SIMS imaging in combination with repeated sputter cycles that erode the sample in a layer-by-layer fashion and thereby make the inner

structure of the cells accessible for SIMS analysis. It is possible to detect intact molecules up to a m/z ratio of 800. However, our analysis does not include larger molecules such as proteins. MALDI-MS is capable of providing the distribution of intact proteins in tissue slices.[17–19] Thus, in terms of accessible mass range MALDI-MS is superior to TOF-SIMS. However, for imaging and 3D applications TOF-SIMS proves to be more advantageous.

The lateral resolution of our experiments was 350 nm and makes it possible to determine the chemical composition on a subcellular level and may be further improved. For instance, Kollmer has reported a lateral resolution of 150 nm when an organic dye was imaged by TOF-SIMS.[3] We estimate the axial (vertical) resolution in our setup to be approximately 100 nm, since microscopic images revealed that NRK cells are on average 6 μm in height and it took typically 60 sputter cycles to remove the cell bodies from the surface. The ultimate depth resolution obtained for depth profiling of organic material in SIMS is currently 30 nm.[7] For comparison, MALDI-MS typically offers a lateral resolution of 50 μm, limited by the focus of the desorbing and ionizing laser beam. The axial resolution of MALDI-MS was determined by the thickness of the tissue slides and was reported to be 50 μm.[20]

In this study we have focused our attention on endogeneous molecular building blocks of animal cells in order validate the 3D TOF-SIMS approach on the well-known cellular architecture. It might be possible in the future to disclose the subcellular storage sites of drugs or other xenobiotics or to trace the fate of endogeneous molecules after pulse chase labeling, provided the compounds studied are detectable by SIMS.

Experimental Section

The epithelial-like NRK cells (normal rat kidney, clone 52E) were grown in Dulbecco's minimum essential medium (Biochrom, Berlin, Germany) supplemented with 10% fetal calf serum (PAA Lab GmbH, Linz, Austria), 2 mM L-glutamine, 100 μg mL^{-1} penicillin, and 100 μg mL^{-1} streptomycin (Seromed, Berlin, Germany). Cultures were kept in incubators with 5% CO_2 atmosphere. For TOF-SIMS experiments the cells were seeded on ordinary No. 1 glass cover slips that had been cleaned and sterilized in an argon plasma for 1 min.

Prior to SIMS analysis the culture medium was aspirated, the cell layer was washed two times with phosphate-buffered saline containing 1 mM Ca^{2+} and 0.5 mM Mg^{2+} (PBS^{++}), and then incubated with 2.5% (v/v) glutaraldehyde in PBS^{++} for 20 min at RT. The aldehyde solution was then replaced by water, and the sample was washed three times. Finally the water was completely aspirated and the sample was allowed to dry at 37 °C for at least 1 h.

3D Microarea data were acquired using a TOF.SIMS 5 instrument (ION-TOF, Germany) equipped with a bismuth primary-ion source and a C_{60}^+ sputter-ion source. Sputtering by C_{60}^+ was performed on a $300 \times 300\ \mu m^2$ area at an energy of 10 keV. The current on the target ranged between 0.6–2.5 nA. The timing scheme consisted of a sputter cycle of 2 s followed by an acquisition of 7 scans in imaging mode in the respective crater center. Sample imaging was performed within an area of $90 \times 90\ \mu m^2$ at 25 keV using Bi_3^+ cluster ions. Each scan provides an image with 256×256 pixels. The target current was 0.1 pA. The focus of the primary-ion beam was optimized to 300 nm with a cycling time of 100 μs making it possible to analyze the m/z range from 1 to 800. Mass-resolved images were recorded at nominal mass resolution, whereas the spectrum shown in Figure 4 was recorded with high mass resolution ($m/\Delta m_{fwhm} > 5000$). Spectra with high mass resolution were used for peak assignment. Data evaluation was performed using the software TOFSIMS 4.1 (ION-TOF GmbH, Germany).

Received: October 31, 2006
Revised: February 14, 2007
Published online: June 5, 2007

Keywords: analytical methods · cell imaging · mass spectrometry · surface analysis

[1] A. Benninghoven, F. G. Rüdenauer, H. W. Werner, Wiley, New York, **1987**, p. 761.
[2] J. C. Vickerman in *ToF-SIMS—Surface Analysis by Mass Spectrometry* (Eds.: J. C. Vickerman, D. Briggs), IMPublications, Manchester/Chichester, **2001**.
[3] F. Kollmer, *Appl. Surf. Sci.* **2004**, *231–232*, 153.
[4] A. M. Belu, D. J. Graham, D. G. Castner, *Biomaterials* **2003**, *24*, 3635.
[5] A. Brunelle, D. Touboul, O. Laprevote, *J. Mass Spectrom.* **2005**, *40*, 985.
[6] B. Hagenhoff, *Mikrochim. Acta* **2000**, *132*, 259.
[7] M. S. Wagner, *Anal. Chem.* **2005**, *77*, 911.
[8] N. Davies, D. Weibel, P. Blenkinsopp, N. Lockyer, R. Hill, J. C. Vickerman, *Appl. Surf. Sci.* **2003**, *203–204*, 223.
[9] S. C. C. Wong, R. Hill, P. Blenkinsopp, N. P. Lockyer, D. Weibel, J. C. Vickerman, *Appl. Surf. Sci.* **2003**, *203–204*, 219.
[10] D. E. Weibel, N. Lockyer, J. C. Vickerman, *Appl. Surf. Sci.* **2004**, *231–232*, 146.
[11] J. Cheng, N. Winograd, *Anal. Chem.* **2005**, *77*, 3651, 77.
[12] E. Niehuis, T. Grehl in *TOF-SIMS: Surface Analysis by Mass Spectrometry* (Eds.: J. C. Vickerman, D. Briggs), IM Publications, Charlton, **2001**, p. 753.
[13] M. Hoppert, A. Holzenburg, *Electron Microscopy in Microbiology*, BIOS Scientific Publishers, Oxford, **1998**.
[14] K. V. Prasanth, D. L. Spector in *Encyclopedia of Life Sciences*, Wiley, Chichester, **2006**.
[15] H. F. Arlinghaus, M. Fartmann, C. Kriegeskotte, S. Dambach, A. Wittig, W. Sauerwein, D. Lipinsky, *Surf. Interface Anal.* **2004**, *36*, 698.
[16] J.-L. Guerquin-Kern, T.-D. Wu, C. Quintana, A. Croisy, *Biochim. Biophys. Acta Gen. Subj.* **2005**, *1724*, 228.
[17] P. Chaurand, M. E. Sanders, R. A. Jensen, M. Caprioli, *Am. J. Pathol.* **2004**, *165*, 1057.
[18] P. Chaurand, M. Stoeckli, R. M. Caprioli, *Anal. Chem.* **1999**, *71*, 5263.
[19] M. Stoeckli, P. Chaurand, D. E. Hallahan, R. M. Caprioli, *Nat. Med.* **2001**, *7*, 493.
[20] A. C. Crecelius, D. S. Cornett, R. M. Caprioli, B. Williams, B. M. Dawant, B. Bodenheimer, *J. Am. Soc. Mass Spectrom.* **2005**, *16*, 1093.

